Compartive Study of Sea Ice Concentration by Using DMSP SSM/I, Aqua AMSR-E and Kompsat-1 EOC

Hyangsun Han and Hoonyol Lee
Department of Geophysics
Kangwon National University
192-1 Hyoja-Dong, Chuncheon, Kangwon-Do 200-701, Republic of Korea
imakdong@kangwon.ac.kr, hoonyol@kangwon.ac.kr

***Abstract*—Satellite passive microwave radiometers such as DMSP SSM/I and Aqua AMSR-E have been providing scientific evidences of sea ice fluctuations through the analysis of decadal archives of daily sea ice concentration (SIC). To evaluate SIC we observed sea ice with a 6 m resolution optical EOC sensor onboard Kompsat-1. Total 68 cloud-free scenes were obtained across the Antarctic continental edges from September to November 2005. In EOC images, we classified sea ice types into White ice (W), Grey-ice (G), and Dark-grey ice (G) and then compared with DMSP SSM/I and Aqua AMSR-E SIC products. In Antarctic springtime, EOC (W+G) SIC showed best fit to SSM/I SIC while (W+G+D) SIC to AMSR-E SIC. It is suggested that SSM/I SIC responds to young ice in addition to multi-year ice and first-year ice, while AMSR-E SIC detects new ice as well.**

Keywords-passive microwave; sea ice concentration; Kompsat-1 EOC; young ice; new ice

I. INTRODUCTION

Polar region is very sensitive to global climatic and environmental changes. The rapid decrease of sea ice extent and the rise of sea level have been reported as prime indicators of climate change possibly from global warming [1], [2].

Since early 1970s, passive microwave (PM) sensors have been widely used for satellite remote sensing of polar region because they are less affected by atmospheric condition or solar radiation. Observations of sea ice by Nimbus-5 ESMR and Nimbus-7 SMMR were succeeded by SSM/I onboard DMSP satellites and AMSR-E onboard Aqua, producing the daily sea ice concentration (SIC) products since 1987 and 2002, respectively [3], [4].

More than two decadal archives of SIC of polar region have been used to study secular variations and fluctuations of sea ice extent and area [5]. Although PM sensors are typically of low resolution (several tens of km), they were efficient for sea ice monitoring because of the homogeneous and continuous observational capability over the entire polar region in daily basis [6].

For the calculation of SSM/I SIC, NASA Team Algorithm (NTA) and Bootstrap Algorithm (BTA) exist. NASA Team2 Algorithm (NT2A) was initially developed for SSM/I as well, and is being used a standard algorithm for AMSR-E. Many studies have focused on calibration and evaluation of such algorithms and reported the disagreement of SICs between PM sensors and other sensors especially for thin ice areas. Most of them, however, used low- (>100 m) to mid-resolution (>30 m) satellite images such as SAR [7], Landsat TM/ETM+ [4], [8], Terra/Aqua MODIS [9], and NOAA AVHRR [10]. Higher resolution sensors would be more favorable to observe various ice types, snow cover, cracks and leads mixed in a relatively small region. Although there exist several satellite sensors of up to sub-meter resolution available commercially or scientifically, few studies have used them for polar research due to their high cost, low success rate of obtaining cloud-free images, and low sun elevation.

In this paper, we report the evaluation results of SSM/I SIC derived from NTA and AMSR-E SIC from NT2A by using 6 m resolution optical images of the Antarctic sea ice obtained by EOC (Electro-Optical Camera) onboard Kompsat-1 (Korea Multi-Purpose SATellite-1). We classified various ice types in EOC images, calculated SIC of each ice types, and compared with SSM/I and AMSR-E SIC.

II. DATA AND PROCESSING

Launched in 1999, Kompsat-1 is the first earth-observing satellite of Korea with EOC as a major payload. EOC is a 6 m resolution, panchromatic, push-broom sensor with 18 km swath and the data storage of up to two minute's imaging (800 km) in ascending polar orbit. During September to November 2005, we obtained 676 scenes from 11 orbits along the Antarctic continental edges. Among them, only 68 cloud-free scenes from 4 orbits could be used for further analysis (Table 1, Fig. 1a). As the weather condition was not taken into consideration during the orbit selection process, it could be said that the success rate of obtaining cloud-free image in this season was just over 10%.

TABLE 1. LIST OF KOMPSAT-1 EOC IMAGES OF THE ANTARCTIC

Orbit Number	Date	Total Scenes	Cloud-free Scenes
1	2005/09/25	60	14
2	2005/10/05	61	40
3	2005/10/08	61	5
4	2005/11/04	63	9
Total		245	68

This research was supported by KOPRI (Korea Polar Research Institute) Grant PE06020.

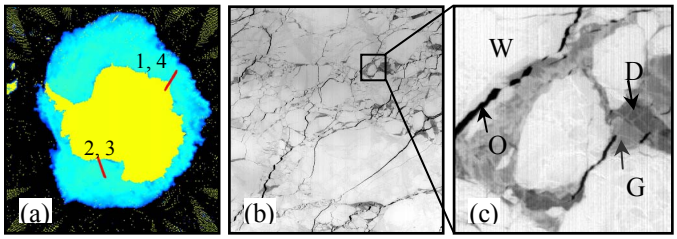

Figure 1. (a) Kompsat-1 EOC orbits overlying SSM/I sea ice concentration image of the Antarctic on 25 Sep. 2005 (7600 km×8300 km). (b) An example of EOC scene of the Antarctic sea ice taken on 5 Oct. 2005 (18 km×18 km). (c) Classification example of EOC ice types into W, G, D, and O (1.8 km×1.8 km).

The EOC images were first geo-coded by using the ephemeris data of Kompsat-1. Geo-location errors of about 5 km was found and corrected by using Terra/Aqua MODIS images that were obtained at close time and locations of EOC images, thus keeping the error within 1 km. This was accurate enough for the comparison of EOC images with PM data that has tens of km-resolution.

Fig. 1(b) and (c) show an example of sea ice by EOC taken on 5 October 2005. It was springtime in the Antarctic when sea ice began to melt slowly after peak expansion of ice regime. Sea ice blocks that were thickened during winter were mostly covered with snow. Leads were filled by refrozen thin ice with little snow ice cover while narrow cracks exposed open water.

Sea ice types are classified into multi-year ice, first-year ice, young ice, and new ice, according to ice thickness, form, and age [11]. Multi-year ice is the one that survived a summer-melt and is thicker than 2-3 m. First-year ice is a yearly ice and is thicker than 30 cm. Multi-year and first-year ice appear bright white due to its thickness, brine pockets and snow cover. Young ice appears grey to grey-white and is thicker than 10 cm, while new ice includes dark nilas, frazil ice, or grease ice that appears dark to dark-grey and is thinner than 10 cm.

As we have no *in situ* ice thickness data, we setup new-sea ice classes such as White ice (W), Grey ice (G), Dark-grey ice (D), and Open water (O), according to grey-level, texture, and morphology of sea ice in EOC images. As most of the Antarctic multi-year ice exists only in the Weddell Sea that was not imaged by EOC in this study, we postulated that W in the EOC images is the first-year ice type. However, thinner ice with heavy snow cover may look white as well. Without ice thickness data, young ice or new ice with heavy snow cover may be classified into W as well EOC images. Contrarily, when sea ice looks grey or dark-grey, we can positively exclude them as being multi-year ice or first-year ice. This is because they must have formed relatively recently, say, within a few days, with little time for snow accumulation. Therefore, G and D, especially of refrozen ice in the leads and cracks, could be positively identified as young ice and new ice.

For the classification of ice types in EOC images, we applied supervised classification using maximum likelihood method and corrected the results by visual inspection (Fig. 1c). EOC SIC of each ice types were calculated by dividing the areas of each ice type by total area so that it could be compared with the results by SSM/I and AMSR-E SICs.

SSM/I is a PM composed of 19.3, 37.0, 85.5 GHz dual polarized channels and 22.2 GHz vertically polarized channel that measure radiation intensity of sea ice. The daily SSM/I SIC product of the Antarctic used in this study is from NTA with 25 km resolution and is the sum of ice type A and B (multi-year ice and first-year ice for the case of the Arctic) [12]. SSM/I SIC were the value of daily average obtained from several orbits of satellites. AMSR-E is also a PM sensor composed of 6.9, 10.7, 18.7, 23.8, 36.5, 89.0 GHz, all in dual polarized channels. AMSR-E also provides the daily SIC of the Antarctic with 12.5 km resolution, calculated from NT2A by summation of ice type A, B and C [13].

We have extracted SSM/I and AMSR-E SICs of the same observation date and location as Kompsat-1 EOC to compare with. We also calculated the Spatio-Temporal STandard Deviation (ST-STD) of SIC in each pixel using 3×3×3 cubic pixel window that comprises the days before and after, and neighboring pixels to see the temporal stability and spatial homogeneity of the SIC. As the daily SSM/I and AMSR-E SIC are calculated by temporal averaging of values from several orbits, direct comparison of them with EOC images obtained in a snap-shot passion could yield significant errors caused by rapid movement of sea ice, changes of sea ice surface state, and geo-location process. Therefore, ST-STD would provide a valuable criterion on the fidelity of comparative data interpretation.

III. Comparison of Eoc and Passive Microwave SICs

We have compared various combinations of EOC SIC of W+G+D, W, and W+G and with SSM/I (Fig. 2a-c) and AMSR-E SIC (Fig. 2d-f). Most of SICs in the Antarctic springtime were higher than 70%. Vertical error bar of each data point indicates the ST-STD of SIC from PM sensors. The black points were the SICs with ST-STD less than 2.5%, which could be considered that sea ice was temporally stable and spatially homogeneous and that we can compared SIC from EOC and PM sensors directly. White data points indicate ST-STD value more than 2.5%. The sea ice state on these points was temporally unstable and spatially inhomogeneous, and the direct comparison of EOC and passive microwave SIC could be biased, rendering it less significant for data interpretation.

SSM/I SIC have lower value than the EOC (W+G+D) SIC as shown in Fig. 2a with the correlation coefficient of 0.717. It is obvious that SSM/I SIC does not respond to all types of sea ice observed by EOC. The comparison of SSM/I SIC with EOC (W) SIC showed very poor match indicating that SSM/I SIC includes more ice types than W (Fig. 2b). When we compared SSM/I SIC with EOC (W+G; excluding D) SIC, the best match was accomplished with the correlation coefficient of 0.830 (Fig. 2c). Therefore, we could conclude that SSM/I SIC responds to W and G, but not to D.

Meanwhile, AMSR-E SIC was best correlated with EOC (W+G; excluding D) SIC (Fig. 2f). However, when we evaluated the black data points, AMSR-E SIC showed better match with EOC SIC of all ice types (W+G+D) as shown in Fig. 2d

Fig. 2 also shows that ST-STD of AMSR-E SIC is lager than that of SSM/I SIC. It is postulated that AMSR-E SIC

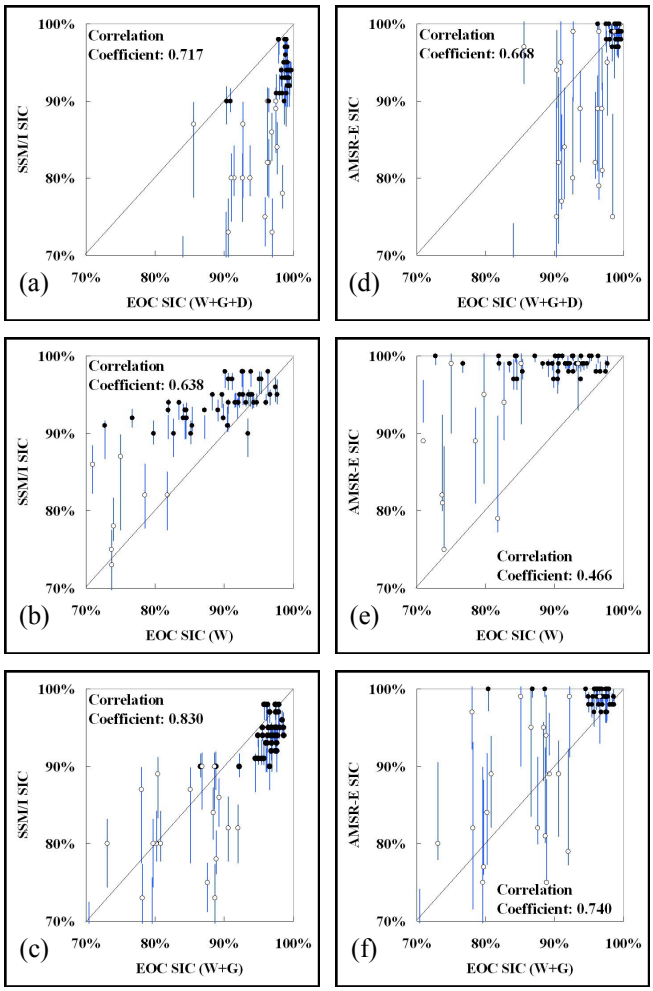

Figure 2. The relationship between (a-c) EOC SIC and SSM/I SIC and (d-f) EOC SIC and AMSR-E SIC in Antarctic springtime, 2005. Black dots are SICs with standard deviation (vertical error bar) less than 2.5% SICs while white dots otherwise. SSMI SIC corresponds well with EOC SIC of W+G in (c), while AMSR-E SIC with EOC SIC of W+G+D in (d), indicating that AMSR-E SIC responds to dark grey ice type in addition to white and grey ice.

responds to D that varies more rapidly than W and G type. This is because D experiences daily thawing and refreezing process in this Antarctic springtime, and its mobility driven by current or wind is relatively high, resulting in higher ST-STD of AMSR-E SIC than that SSM/I SIC.

Through the comparison of SICs from EOC and PM sensors so far, it was found that both SSM/I and AMSR-E respond G as well as W. This is somewhat controversial to the NTA and NT2A that were known to respond only to the multi-year ice and first-year ice stages. Instead, they seem to respond to the G types as well that is similar to young ice. It was also found that AMSR-E SIC includes D as well while SSM/I SIC does not.

IV. Effect of Dark-Grey Ice on Passive Microwave Sensors

Fig. 3a shows the relationship between the AMSR-E and SSM/I SIC values that were used for comparison with EOC

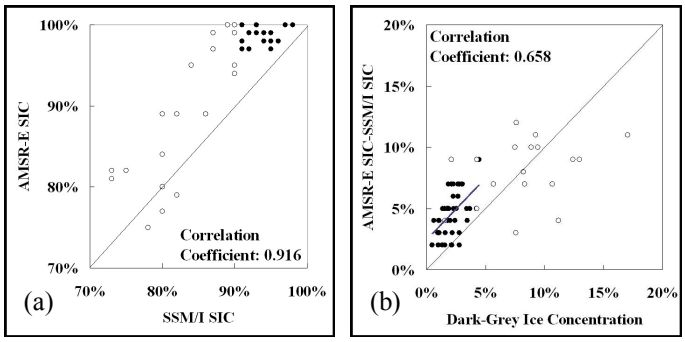

Figure 3. Effects of EOC dark-grey ice to AMSR-E and SSM/I. (a) Comparison of SSM/I SIC and AMSR-E SIC of the Antarctic. (b) The relationship between EOC (D) SIC and the difference of AMSR-E SIC and SSM/I SIC.

images. Again, the black dots represent the values with ST-STD less than 2.5%. It shows that most AMSR-E SIC values higher than SSM/I SIC by almost 5% in average. The difference came from the fact that the SSM/I NTA discriminates ice type A and B while NT2A detects ice type C additionally. Comiso *et al*. [14] reported that ice type C has inhomogeneous surface layer with significant complex scattering that frequently underestimated by NTA. The seeming characteristic of ice type C is presumed similar to ice thin ice but they are not the exact match. Heinrichs *et al*. [15] used term 'thin ice', instead of ice type C for this reason. To see what type of EOC SIC is comparable to ice type C, we compared various types of EOC SICs of G, D, and G+D with the difference between AMSR-E SIC and SSM/I SIC. Among them, EOC (D) SIC was best correlated with the difference of AMSR-E and SSM/I SIC with correlation coefficient of 0.658 (Fig. 3b). Considering the black dots with ST-STD less than 2.5% only, EOC (D) SIC has strong positive relationship with the ice type C of AMSR-E NT2A.

Fig. 4 shows examples of EOC images with different portion of dark-grey SIC. Dark-grey ice in EOC image seem to be the recently-frozen thin ice layer composed of grease ice, dark nilas or frazil ice with no snow cover. Fig. 4a is an EOC image obtained on 25 September 2005, which comprises 51.8% of W, 29.0% of G, and 13.0% of D. SSM/I and AMSR-E SIC of this image were 80% and 89%, respectively, showing 9% of difference that is similar to EOC (D) SIC. Fig. 4b is

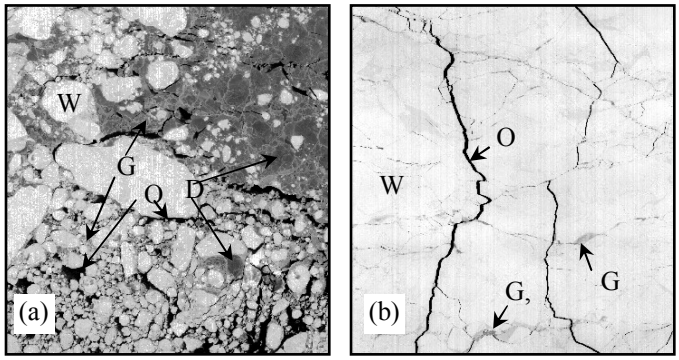

Figure 4. Two examples of EOC scenes (18 km×18 km) with different ice concentrations. (a) EOC image with large portion of dark-grey ice (W: 51.8%, G: 29.0%, D: 13.0%, O: 6.2%) taken on 25 September 2005 (SSM/I: 80%, AMSR-E: 89%). (b) EOC image with little dark-grey ice (W: 97.4%, G: 1.0%, D: 0.5%, O: 1.1%) taken on 5 October 2005 (SSM/I: 96%, AMSR-E: 98%).

another example of EOC image with little dark-grey ice type, acquired on 5 October 2005. The scene includes 97.4% of W, 1.0% of G, and 0.5% of D. SSM/I and AMSR-E SIC were 96% and 98%, respectively, showing 2% of difference between PM SICs.

From above discussions, we could confirm that dark-grey ice is similar to ice type C defined in NT2A and is responsible for the difference between AMSR-E and SSM/I SIC.

V. CONCLUSION

Analysis of total 68 cloud-free scenes of sea ice in the Antarctic springtime by Kompsat-1 EOC sensor proved that high resolution optical satellite images are useful in classifying detailed ice types such as White ice (W), Grey ice (G), and Dark-grey ice (D), and in evaluating the daily sea ice concentration (SIC) products derived by SSM/I and AMSR-E.

Comparison of EOC with passive microwave sensors showed that SSM/I SIC calculated by NASA Team Algorithm (NTA) responds not only to W but also to G, but not to D, while AMSR-E SIC calculated by NASA Team2 Algorithm (NT2A) can see D as well. Sea ice types can be defined differently from different observation methods one may have used, and could not be homologous to each other. However, this study suggests that SSM/I SIC responds not only to multi-year ice and first-year ice but also to young ice, while AMSR-E SIC includes new ice as well. It is also suggested that new ice is the major source of difference between SSM/I and AMSR-E SIC, and is analogous to the ice type C defined in AMSR-E NT2A.

Despite the absence of ground reference data such as ice thickness or surface condition at the time of satellite data acquisition, we could evaluate the different characteristics of SSM/I and AMSR-E SIC by using the high resolution optical EOC images. More detailed evaluation and assessment of passive microwave SIC data in various season and locations would be essential to link them to the study of global environment change. This could be possible by the continuous archiving efforts of high resolution optical images in addition to active microwave sensors such as SAR or altimeter and in situ data collection.

ACKNOWLEDGMENT

This research was supported by KOPRI (Korea Polar Research Institute) Grant PE06020. The Kompsat-1 EOC dataset were provided by KARI (Korea Aerospace Research Institute). SSM/I and AMSR-E data were obtained from EOS (Earth Observing System) data gateway at NSIDC (National Snow and Ice Data Center).

REFERENCES

[1] P. Gloersen, C. L. Parkinson, D. J. Cavelieri, J. C. Comiso, and H. J. Zwally, "Spatial distribution of trends and seasonaliry in the hemispheric sea ice civers: 1978-1996," *J. Geophys. Res.*, vol. 104, pp. 20,827-20,836, 1999.

[2] C. L. Parkinson, D. J. Cavalieri, P. Gloersen, H. J. Zwally, and J. C. Comiso, "Arxtic sea ice extents, areas, and trends, 1978-1996", *J. Geophys. Res.*, vol. 104, pp. 20,837-20,856, 1999.

[3] D. J. Cavalieri, P. Gloersen, C. L. Parkinson, J. C. Comiso, and H. J. Zwally, "Observed hemispheric asymmetry in global sea ice changes", *Science*, vol. 278, pp. 1104-1106, 1997.

[4] D. J. Cavalieri, T. Markus, D. K. Hall, A. J. Gasiewski, M. Klein, and A. Ivanoff, "Assessment of EOS Aqua AMSR-E arctic sea ice concentration using Landsat-7 and airborne microwave imagery", *IEEE Trans. Geosci. Remote Sensing*, vol. 44, pp. 3057-3069, 2006.

[5] E. Bjørgo, O. M. Johannessen, and M. W. Miles, "Analysis of merged SMMR-SSMI time series of Arctic and Antarctic sea ice parameters 1978-1995", *Geophys. Res. Lett.*, vo. 24, pp. 413-416, 1997.

[6] D. J. Cavalieri, C. L. Parkinson, P. Gloersen, J. C. Comiso, and H. J. Zwally, "Deriving long-term time series of sea ice cover from satellite passive-microwave multisensor data sets", J. Geophy. Res., vol. 104, pp. 15,803-15,814, 1999.

[7] G. I. Belchansky, and D. C. Douglas, "Seasonal comparisons of sea ice concentrations estimates derived from SSM/I, OKEAN, and RADARSAT data", *Remote Sens. Environ.*, vol. 81, pp. 67-81, 2002.

[8] A. P. Worby, and J. C. Comiso, "Studies of the Antarctic sea ice edge and ice extent from satellite and ship observations", *Remote Sens. Environ.*, vol. 92, pp. 98-111, 2004.

[9] C. Drüe, and G. Heinemann, "Accuracy assessment of sea-ice concentrations from MODIS using in-situ measurements, *Remote Sens. Environ.*, vol. 95, pp. 139-149, 2005.

[10] W. J. Emery, C. Fowler, and J. K. Maslanik, "Arctic sea ice concentrations from special sensor microwave imager and advanced very high resolution radiometer satellite data", *J. Geophy, Res.*, vol. 99, pp. 18,329-18,342, 1994.

[11] World Meteorologocal Organization, "WMO-sea ice nomenclature", 1970 ed., WMO series no. 259, Secretariat of the World Meteorological Organization, Geneva, 1970.

[12] J. C. Comiso, D. J. Cavalieri, C. L. Parkinson, and P. Gloersen, "Passive microwave algorithms for sea ice concentration: A comparison of two techniques", *Remote Sense. Environ.*, vol. 60, pp. 357-384, 1997.

[13] T. Markus, and S. T. Dokken, "Evaluation of late summer passive microwave Arctic sea ice retrievals", *IEEE Trans. Geosci. Remote Sensing*, vol. 40, pp. 348-356, 2002.

[14] J. C. Comiso, D. J. Cavalieri, and T. Markus, "Sea ice concentration, ice temperature, and snow depth using AMSR-E data", *IEEE Trans. Geosci. Remote Sensing*, vol. 41, pp. 243-252, 2003.

[15] J. F. Heinrichs, D. J. Cavalieri, and T. Markus, "Assessment of the AMSR-E sea ice concentration product at the ice edge using RADARSAT-1 and MODIS imagery", *IEEE Trans. Geosci. Remote Sensing*, vol. 44, pp. 3070-3080, 2006.